

Accepted Manuscript

Title: Olefin hydroformylation and kinetic studies using mono- and trinuclear *N,O*-chelate rhodium(I)-aryl ether precatalysts

Authors: Shepherd Siangwata, Nicholas C.C. Breckwoldt, Neill J. Goosen, Gregory S. Smith



PII: S0926-860X(19)30334-5
DOI: <https://doi.org/10.1016/j.apcata.2019.117179>
Article Number: 117179

Reference: APCATA 117179

To appear in: *Applied Catalysis A: General*

Received date: 30 April 2019
Revised date: 11 July 2019
Accepted date: 26 July 2019

Please cite this article as: Siangwata S, Breckwoldt NCC, Goosen NJ, Smith GS, Olefin hydroformylation and kinetic studies using mono- and trinuclear *N,O*-chelate rhodium(I)-aryl ether precatalysts, *Applied Catalysis A, General* (2019), <https://doi.org/10.1016/j.apcata.2019.117179>

This is a PDF file of an unedited manuscript that has been accepted for publication. As a service to our customers we are providing this early version of the manuscript. The manuscript will undergo copyediting, typesetting, and review of the resulting proof before it is published in its final form. Please note that during the production process errors may be discovered which could affect the content, and all legal disclaimers that apply to the journal pertain.

Olefin hydroformylation and kinetic studies using mono- and trinuclear *N,O*-chelate rhodium(I)-aryl ether precatalysts

Shepherd Siangwata,^a Nicholas C. C. Breckwoldt,^b Neill J. Goosen,^b Gregory S. Smith^{a*}

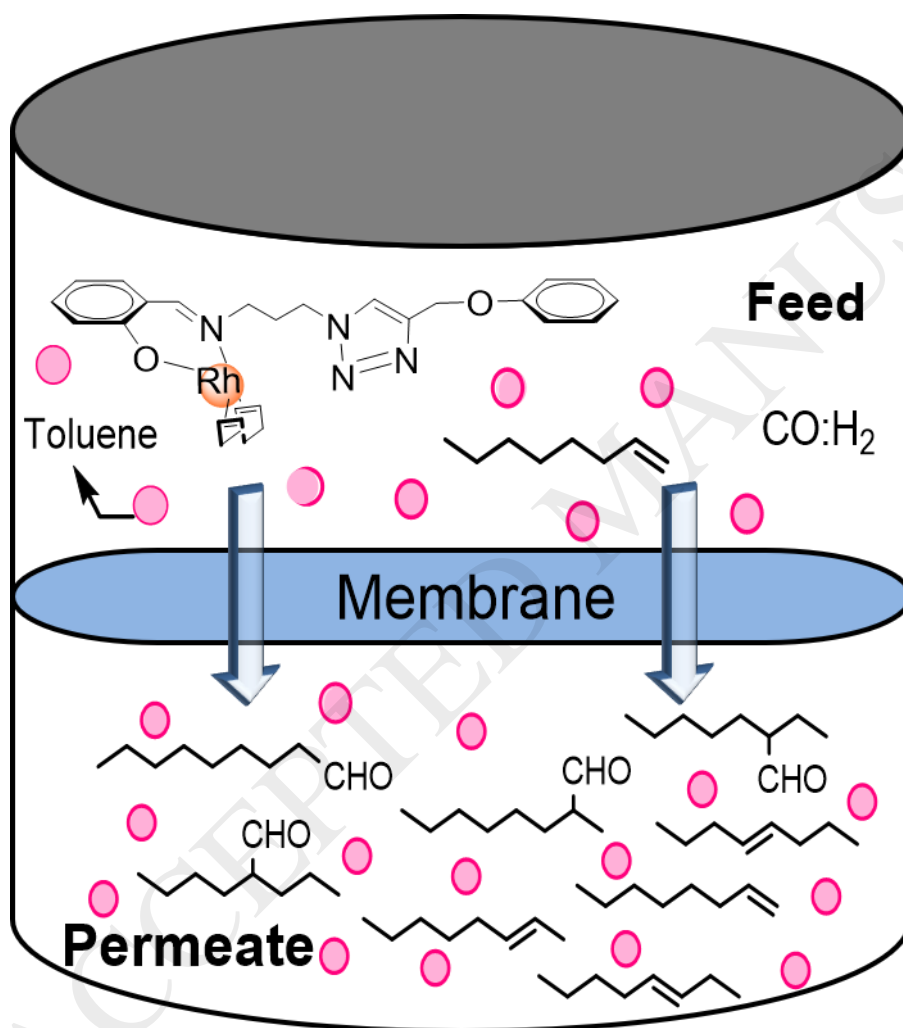
^aDepartment of Chemistry, University of Cape Town, Rondebosch, 7701, South Africa.

^bDepartment of Process Engineering, Stellenbosch University, Private Bag X1, Matieland, 7602, South Africa

* Corresponding author. Tel.: +27 (0)21 650 5279

E-mail address: gregory.smith@uct.ac.za

Graphical abstract



Highlights

- Rhodium-salicylaldehyde precatalysts evaluated for olefin hydroformylation.
- Catalysts can be reused using organic solvent nanofiltration.
- Both catalysts have an activation of 62 kJ mol⁻¹.
- Observed rate constants compare favourably with a modified rate model.

ABSTRACT

Rh(I)-salicylaldimine-triazole mononuclear (**6**) and trinuclear (**7**) complexes based on an aryl-ether scaffold were investigated as precatalysts in the rhodium-catalysed hydroformylation of the terminal olefin, 1-octene, and internal olefins, 7-tetradecene and 4-octene. The complexes generally show good catalytic activity in the hydroformylation of 1-octene at temperatures ranging from 75 °C to 95 °C and syngas pressures of 20 to 40 bar. The precatalysts have excellent stability and could be reused several times using organic solvent nanofiltration under optimum conditions of 85 °C and 40 bar. Kinetic studies using catalyst precursor **6** were investigated by evaluating the effect of temperature, syngas total pressure and catalyst loading on the rate of hydroformylation. The activation energy for the hydroformylation of 1-octene was calculated to be 62 kJ mol⁻¹ and the experimental rate constants were found to be in good agreement with the predicted rate data obtained using a modified fundamental mechanism-based rate model.

Keywords: hydroformylation; olefins; rhodium; nanofiltration; kinetics

1. Introduction

The hydroformylation reaction is a metal-catalysed reaction, involving the addition of carbon monoxide and hydrogen to alkenes to produce aldehydes. This atom efficient reaction, also known as the “Oxo process” is the largest homogeneous transition metal complex-catalysed reaction in industry, producing over 14 million tons of aldehydes annually [1–4]. Subsequent transformation of these aldehydes (linear or branched) leads to “oxo intermediates” which are further processed into downstream products mainly used in the pharmaceutical, detergent and agrochemical industries. The widely used metal of choice is rhodium owing to its good catalytic activity and selectivity for aldehydes under mild reaction conditions (typically, 80 – 100 °C and 10 – 25 bar) [5,6]. However, the use of rhodium-based catalyst precursors in hydroformylation, like most homogeneous catalytic systems, is hampered by separation of the catalyst from the products. The presence of residual metal in the product stream often comes with huge financial implications that impacts on several fields. Separation of the metal from the products through the conventional distillation methods is only suitable for low boiling point short chain alkenes, since the high temperatures that are required for long chain alkenes often leads to catalyst decomposition and subsequently low catalyst activity

[7]. Several strategies have been used to facilitate the recovery of homogeneous catalysts in hydroformylation, while maintaining the high activity and selectivity of the rhodium-based catalyst precursors. These strategies mainly involve the immobilisation of a catalyst on a solid support (polymers), as well as heterogenization of a catalyst in a different phase to that of the reactants and products (biphasic catalysis) [8][9–18]. A less explored, though highly attractive recovery technique is the use of membrane technology which allows permeation through the membrane by selected molecules upon application of a driving force. The permeation of membranes is easily tuneable by manipulating the various physicochemical properties of both the membrane (pore size, material, thickness and diameter) and the constituents of the feed (molecular weight, polarity, geometry, viscosity and surface tension) [19–24]. A noteworthy strategy in membrane technology is the organic solvent nanofiltration technique (OSN), which entails the use of nanofiltration membranes to separate molecules present in organic solvents without the need for processes that are catalyst-destructive or that require high-energy [25–32]. This is considered a greener approach towards homogeneous catalyst recovery because of its relatively low energy requirements and facile catalyst separation without the need for biphasic media. These membranes are also deemed user-friendly and the whole process can be readily scaled up. Moreover, the OSN recovery technique is highly successful when the catalyst is of high molecular weight relative to the other constituents of the feed. This allows for the determination of the molecular weight cut-off (MWCO), which is the molecular weight at which the membrane will achieve 90% rejection/retention [33]. Since homogeneous catalysts (such as those used for hydroformylation) are usually of the same molecular weight as the reagents and products, molecular weight enlargement (MWE) of the catalyst can facilitate efficient membrane filtration. Various soluble supports have been used for molecular weight enlargement of homogeneous catalysts, and these include polyhedral oligomeric silsesquioxanes (POSS), polymers and dendrimers [34–36]. When metals are incorporated into dendritic arms of the support, the resulting metallodendrimers often possess enhanced catalytic activity due to the multiple catalytic sites that propagate from the core [37–39]. These mimic naturally occurring metalloenzymes, which often possess improved catalytic efficiency over their mononuclear analogues owing to multiple active sites. From a Green Chemistry perspective, there are huge gains through a catalytic system that can offer excellent efficiency with facile catalyst recovery for multiple reuse.

Herein, we report on the synthesis and application of mono- and trinuclear complexes of Rh(I) as catalyst precursors in the hydroformylation of a linear α -olefin and internal olefins. The recovery of these complexes using the OSN technique, as well as their kinetic studies in the hydroformylation of 1-octene, is evaluated.

2. Experimental

2.1 General

All chemicals and solvents were reagent grade and used as received from Sigma-Aldrich, unless otherwise stated. *N*-3-Bromopropylsalicylaldehyde [40], phenyl propargyl ether (**2**) [41] and 1,1,1-tris(4-propargyl ether phenyl)ethane (**3**) [42] were prepared according to modified previously reported literature procedures. RhCl₃·3H₂O was purchased from Heraeus South Africa (Pty) Ltd. 7-Tetradecene was prepared via the metathesis of 1-octene using the Hoveyda–Grubbs second generation pre-catalyst, and then purified by removing the metathesis catalyst via organic solvent nanofiltration. The unreacted 1-octene was then boiled off to yield 7-tetradecene in high purity (>98%) [43]. Carbon monoxide and hydrogen gas were supplied by Afrox Ltd. Nuclear Magnetic Resonance (NMR) spectra were recorded on either a Bruker Biospin GmbH (¹H: 400.22 MHz; ¹³C: 100.65 MHz) or a Varian XR300 MHz (¹H: 300.08 MHz; ¹³C: 75.46 MHz) spectrometer. NMR values were reported relative to the internal standard tetramethylsilane (δ 0.00). FT-IR spectra were recorded using Attenuated Total Reflectance Infrared spectroscopy (ATR-IR). Melting points were determined using a BÜCHI melting point apparatus B-540. Mass spectrometry was carried out using a Waters API Quattro Micro Triple Quadrupole electrospray ionisation mass spectrometer in the positive-ion mode. The mobile phase for LCMS analyses was prepared using solvents and reagents of HPLC-grade obtained from Sigma-Aldrich (ammonium acetate as an additive), Merck (glacial acetic acid) and Microsep (acetonitrile and methanol). Low Resolution-ESI-MS was acquired on an Agilent 1260 Infinity HPLC system (Agilent® 1260 Infinity Binary Pump, Agilent® 1260 Infinity Diode Array Detector (DAD), Agilent® 1290 Infinity Column Compartment, and Agilent® 1260 Infinity Standard Auto sampler) coupled to Agilent 6120 Quadrupole MS system and Peak Scientific® Genius 1050 Nitrogen Generator. Phenomenex Kinetex® 2.6 μ m EVO C18 100 Å (30 x 2.1 mm) reverse phase analytical column was used. The

chromatographic method included a column temperature of 40 °C, an injection volume of 2 µL, flow rate of 0.7 mL/ min and maximum column back pressure set at 600 bars. The mass spectrum was acquired using electrospray ionisation (ESI) in the positive ionization mode. Analyses and quantification of the catalytic products was carried out using a Perkin Elmer Clarus 580 GC instrument equipped with a flame ionisation detector and 30m capillary column. All spectroscopic and analytical data is supplied in the Supplementary Information.

2.2 Preparation of azidopropyl salicylaldimine (**1**).

NaN₃ (0.303 g, 4.66 mmol) was added to a stirring solution of *N*-3-bromopropylsalicylaldimine (1.03 g, 4.23 mmol) in DMF (5 mL) [44]. The reaction was heated under N₂ at 80 °C overnight. The reaction was then allowed to cool to room temperature and then filtered by gravity. The solvent was removed azeotropically using toluene. The resultant brown crude product was then re-dissolved in ethyl acetate and washed with water (2 x 50 mL) and then with brine solution (3 x 50 mL). The organic layer was collected and dried over magnesium sulfate and filtered by gravity. The solvent was removed from the filtrate to produce **1** as a yellow oil which was dried *in vacuo*.

2.3 Preparation of 4-(phenoxyethyl)-1*H*-1,2,3-triazol-1-yl-propylsalicylaldimine ligand (**4**).

CuI (1.41 x 10⁻² g, 7.41 x 10⁻² mmol) was stirred in DIPEA (1.91 x 10⁻² g, 0.148 mmol) at room temperature for 5 minutes in a 10 mL round bottom flask under N₂ [45]. A mixture of the alkyne phenyl propargyl ether **2** (0.196 g, 1.48 mmol) and the azidopropyl salicylaldimine **1** (0.303 g, 1.48 mmol) was added, and the reaction was left stirring at room temperature under N₂, forming a paste. After 24 hours, the reaction mixture was diluted with dichloromethane (3 mL) to bring the paste into solution and filtered by gravity. The filtrate was washed with saturated NH₄Cl (3 x 50 mL) and the organic layer was then dried over magnesium sulfate and filtered by gravity. The filtrate was reduced to a minimum (*ca.* 2 mL) and added dropwise into rapidly stirring diethyl ether (400 mL), yielding the product as a dull yellow precipitate. Vigorous stirring was

continued for 1 hour to triturate the product, which was collected by vacuum filtration and washed with diethyl ether.

2.4 Preparation of 1,1,1-tris(4-phenoxyethyl)ethane-1H-1,2,3-triazol-1-yl-propylsalicylaldehyde ligand (**5**).

CuI (1.14×10^{-2} g, 5.98×10^{-2} mmol) was stirred in DIPEA (1.54×10^{-2} g, 0.119 mmol) at room temperature for 5 minutes in a 10 mL round bottom flask under N₂ [45]. The alkyne 1,1,1-tris(4-propargyl ether phenyl)ethane **3** (0.168 g, 0.398 mmol) was dissolved in dichloromethane (2 mL) and introduced into the flask, and the mixture was allowed to stir for a further 10 minutes, forming a paste. Azidopropyl salicylaldehyde **1** (0.247 g, 1.21 mmol) was added and the reaction mixture was stirred at room temperature for 72 hours under N₂. Dichloromethane (5 mL) was added, and the mixture was stirred at 45 °C for 1 hour under N₂. The reaction was allowed to cool to room temperature and the mixture was filtered by gravity. The filtrate was collected and filtered through a pad of Celite. The solvent was reduced to a minimum (ca. 2 mL) and added dropwise into rapidly stirring diethyl ether (400 mL) yielding the product as a dull yellow precipitate. Vigorous stirring was continued for a further 30 minutes and the product was collected by vacuum filtration and washed with diethyl ether.

2.5 Preparation of 4-(phenoxyethyl)-1H-1,2,3-triazol-1-yl-propylsalicylaldehyde-based Rh(I) complex (**6**)

The rhodium(I) complexes were prepared following a method reported previously [46]. Triethylamine (1.37×10^{-2} g, 0.135 mmol) was added to a stirring solution of the 4-(phenoxyethyl)-1H-1,2,3-triazol-1-yl-propylsalicylaldehyde ligand **4** (3.50×10^{-2} g, 0.104 mmol) in dichloromethane (5 mL) and the reaction was left stirring for 30 minutes. A half molar equivalent of [RhCl(COD)]₂ (2.56×10^{-2} g, 5.20×10^{-2} mmol) was added and the reaction was left to stir for 24 h at room temperature. The solution was diluted with dichloromethane (15 mL) and washed with distilled water (2 x 30 mL). The organic phase was collected and dried over magnesium sulfate, filtered by gravity and the solvent in the filtrate was reduced to a minimum (ca. 2 mL). Diethyl ether was

added (15 mL) to precipitate the product as a yellow solid which was collected by vacuum filtration and dried *in vacuo*.

2.6 Preparation of 1,1,1-tris(4-phenoxyethyl)ethane-1H-1,2,3-triazol-1-yl-propylsalicylaldehyde-based Rh(I) complex (**7**).

Triethylamine (2.88×10^{-2} g, 0.285 mmol) was added to a stirring solution of the 1,1,1-tris(4-phenoxyethyl)ethane-1H-1,2,3-triazol-1-yl-propylsalicylaldehyde ligand **5** (7.55×10^{-2} g, 7.31×10^{-2} mmol) in dichloromethane (5 mL) and the reaction was left stirring for 30 minutes [46]. A one and a half molar equivalent of $[\text{RhCl}(\text{COD})]_2$ (5.40×10^{-2} g, 0.110 mmol) was added and the reaction was left to stir for 24 h at room temperature. The solution was diluted with dichloromethane (15 mL) and washed with distilled water (2 x 30 mL). The organic phase was collected and dried over magnesium, filtered by gravity and the solvent in the filtrate was then reduced to a minimum (ca. 2 mL). Diethyl ether was added (15 mL) to precipitate the product as a yellow solid which was collected by vacuum filtration and dried *in vacuo*.

2.7 General procedure for the catalytic experiments

Hydroformylation studies were conducted in a 100 mL stainless steel pipe reactor equipped with a Teflon interior. In a typical experiment, the reactor was charged with toluene (7.5 mL), 1-octene (1.21 g, 10.7 mmol), dodecane as the internal standard (100 μL) and **6** (2.87×10^{-4} mmol, substrate : Rh ratio 2500 : 1). The reactor was heated to the desired temperature, flushed with syngas ($\text{CO}:\text{H}_2 = 1:1$) and then pressurised to the appropriate syngas pressure. Samples were analysed after 4 hours using gas chromatography (GC). Authentic iso-octenes and aldehydes, alcohols and *n*-octane were used to confirm the products. Recyclability experiments were carried out after 2 hours using the organic solvent nanofiltration technique (OSN) under the optimised conditions of temperature and pressure. In a typical recovery experiment, after the first catalytic run, the reaction components were cooled to room temperature, and diluted with toluene (7.5 mL). The solution was emptied into a stainless-steel dead-end separation cell mounted with a pre-conditioned Duramem[®] 200 membrane, and the cell was pressurised to 25 bar with nitrogen gas to enable the feed to flow

through the membrane. The permeate was collected over time and the cell was depressurised when the feed was reduced to a minimum. The retentate containing the catalyst was decanted from the cell and re-introduced into the catalytic reactor bearing fresh substrate and toluene. The catalytic reaction was repeated under the same conditions of temperature, pressure and time, and subjected to the OSN technique after each cycle. Kinetic studies on the hydroformylation of 1-octene were conducted using the mononuclear catalyst precursor **6** through varying the temperature, time, catalyst loading and total syngas pressure.

3. Results and discussion

3.1 Synthesis of salicylaldimine-triazole-based mono- and trimeric ligands (**4** and **5**).

The precursor, azidopropyl salicylaldimine ligand (**1**), was prepared by the reaction of *N*-3-bromopropylsalicylaldimine [40], with sodium azide in dimethylformamide to obtain the product as a yellow oil in good yield (89%), (Scheme 1). The precursors to the salicylaldimine-triazole ligands **4** and **5** were prepared via a Williamson ether reaction of propargyl bromide with either phenol or THPE in acetone respectively. The resultant aryl-ether alkyne products were isolated as either a yellow oil (**2**), or a white solid (**3**). Subsequently, the new yellow aryl-ether triazole-based ligands **4** and **5** were prepared in good yields (85% (**4**) and 90% (**5**)) via a diisopropylethylamine-promoted CuI-catalysed azide-alkyne cycloaddition reaction of azidopropyl salicylaldimine **1** with the respective alkyne (**2** or **3**) (Scheme 1). The ¹H NMR spectra of **4** and **5** show diagnostic triazole signals at *ca.* $\delta = 8.25$ (H₁₂), and the imine proton signals (H₈) at *ca.* $\delta = 8.50$ for both compounds (Fig. S1 and Fig. S2). The diagnostic methyl signal of the trimeric core of **5** is observed upfield at $\delta = 2.04$. The infrared spectra confirm formation of **4** and **5** by the presence of absorption bands at *ca.* 3085 cm⁻¹, assigned to the ν (C–H) stretching frequency of the 1,2,3-triazole and characteristic strong imine ν (C=N) absorption bands at *ca.* 1630 cm⁻¹ for both ligands. Additionally, the spectra do not show the absorption bands previously reported for the azido (**1**) [40] and alkyne (**2** and **3**) [40,41] stretching frequencies. This is in line with data reported in the literature for Cu(I)-catalyzed azide-alkyne “click” cycloaddition reactions [47].

3.2 Synthesis of aryl-ether Rh(I)-salicylaldimine-triazole-based mono- and trinuclear complexes (**6** and **7**).

The new aryl-ether Rh(I)-salicylaldimine-triazole-based complexes **6** and **7** were synthesised by deprotonation of the ligands **4** and **5** using triethylamine, and subsequent complexation with the appropriate molar equivalent of the Rh(I) dimer [RhCl(COD)]₂, (COD = 1,5-cyclooctadiene), [46] Scheme 1. The products were isolated as brown solids in good yields (83% (**6**), and 99% (**7**)). The ¹H NMR spectra (Fig. S3 and Fig. S4) show upfield shifts of the imine proton signals from ca. $\delta = 8.50$ in **4** and **5** to $\delta = 8.18$ in **6** and **7**, characteristic of the synergistic effect involving M to L pi-donation and L to M sigma donation. The infrared spectra of both complexes also show shifts of the imine absorption bands to lower wavenumbers upon coordination of the ligands to the metal, corroborating the coordination of the imine nitrogen. This has been reported for similar compounds in the literature [48–51].

3.3 Preliminary screening using precatalyst **6**

Preliminary experiments were performed using the model mononuclear complex (**6**) as the catalyst precursor, and 1-octene as the substrate. The effects of temperature (75 – 95 °C) and pressure (20 – 40 bar) were evaluated in the hydroformylation of 1-octene over 4 hours. Moderate conversion of 1-octene (79%) is observed at the lowest temperature and pressure (75 °C and 20 bar syngas pressure) of this study (Fig. S5). Increasing the temperature (to 85 °C and 95 °C) at a constant pressure of 20 bar results in near-quantitative conversion of 1-octene (>97%), indicative of the energy required for activation of the olefin. A further increase in temperature and pressure has no significant effect on the conversion of 1-octene. A gradual increase in chemoselectivity towards aldehydes is observed with an increase in temperature at constant pressure (20 bar, 75 °C – 95 °C), Figure S6. A further increase in pressure with an increase in temperature results in improved chemoselectivity towards aldehydes of up to 96%. The observed bias towards aldehydes with an increase in syngas pressure and temperature can be ascribed to the hydroformylation of the iso-octenes to aldehydes due to increased CO concentration in solution which limits isomerisation and accelerates the CO migration step [52]. A higher degree of linear

aldehydes (73%) is observed at low conditions of temperature (75 °C) and pressure (20 bar), Figure S7, whereas increasing the temperature and pressure results in a decrease in linear aldehydes, as there exists preferential isomerisation of the terminal olefin at high temperatures, leading to iso-octenes which gradually undergo hydroformylation to form branched aldehydes. This observation is further supported by the *n:iso* ratios in Table 1, which decrease as the temperature is raised from 75 °C to 95 °C. It can be postulated that the tetracarbonyl rhodium species $[\text{Rh}(\text{CO})_4]^+$ may form at higher pressure, and can influence the selectivity of the catalyst. The increase in pressure at constant temperature results in a steady increase in activity from 154 h^{-1} (75 °C/ 20 bar) to 444 h^{-1} (75 °C/ 40 bar). Increasing the temperature to 85 °C at a syngas pressure of 40 bar gives the best activity of 1-octene (554 h^{-1} , entry 6).

3.4 Mercury poisoning experiment

The mercury drop test was carried out to determine if the reaction was entirely homogeneous or may have taken place in the presence of nanoparticles (entry 7, Table 1). A negligible decrease in conversion was observed {from 99% (entry 6) to 93% (entry 7)}, suggesting that it is largely a molecular species that catalyses the reaction and that nanoparticles may contribute to a small extent to the observed transformation of the olefin to the aldehydes, as has been observed in previous studies with similar Rh(I) catalyst precursors [44,47].

3.5 Catalytic evaluation using precatalyst **7**

From the optimisation experiments using catalyst precursor **6**, the best conditions were established at 85 °C and 40 bar, based on the good chemoselectivity for aldehydes (90%), near-quantitative conversion of the substrate (99%) and the high activity (554 h^{-1}). As a consequence of the near complete conversion and to delineate more meaningful results, it was decided to evaluate the trinuclear precatalyst at a reduced syngas pressure. The trinuclear complex (**7**) was successfully tested in the hydroformylation of 1-octene under milder reaction conditions of 85 °C and 20 bar. The dendritic complex (**7**) shows a similar catalyst performance as the mononuclear analogue (**6**) under the chosen conditions of study (Table 2). It is worth noting that the trinuclear complex is less soluble in toluene than the mononuclear complex under the

tested conditions, suggesting a less favourable interaction between the substrate and the catalyst precursor. Previous literature studies report that the poorer solubility of dendritic catalyst precursors in the conventional solvent of choice for hydroformylation (toluene), sometimes lead to less evident dendritic effects [49,50].

3.6 Substrate variation

The substrate scope was extended to the internal olefins 7-tetradecene and 4-octene, which are highly important substrates in the surfactant industry. Hydroformylation of such substrates is generally carried out at high temperatures (>100 °C) owing to the high thermodynamic stability of internal olefins over their terminal counterparts [55–57]. In this study, the experiments were carried out at 120 °C and 40 bar for 4 hours using the mononuclear complex **6** (Table 3).

Good conversions of both substrates were observed (>80%), with catalyst precursor **6** showing good chemoselectivity towards aldehydes (90%) for 7-tetradecene. The relatively shorter carbon chain internal olefin trans-4-octene gave a higher percentage of iso-octenes to aldehydes (82% : 18%, respectively), which could be explained by the relative ease of isomerisation of trans-4-octene compared to 7-tetradecene, which is highly thermodynamically stable. Moreover, minute quantities of 1-octene and nonanal were observed in the hydroformylation of trans-4-octene, indicative of the highly preferential isomerisation of trans-4-octene over hydroformylation.

3.7 Reusability of the catalyst: Organic Solvent Nanofiltration

Catalyst recovery and recyclability was carried out for 2 hours using the organic solvent nanofiltration technique at 85 °C and 40 bar. The separation was achieved by using a stainless-steel dead-end separation cell mounted with a pre-conditioned Duramem® 200 membrane. The choice of the membrane was mainly influenced by the molecular weight cut-off of the membrane (MWCO = 200 g mol⁻¹), in-line with the molecular weight of the catalysts under study (complex **6** = 546.48 g mol⁻¹; complex **7** = 1447.35 g mol⁻¹). The catalyst precursors **6** and **7** maintain good conversion of 1-octene after OSN recovery with each cycle (Fig. 1), with catalyst precursor **6** showing

only a slight decline in conversion (to 91%) after the 4th cycle, indicative of the effectiveness of the OSN membrane in recycling the catalysts. Most remarkably, the catalyst precursors **6** and **7** show good catalytic activity with each cycle (Fig. 2). Both catalyst precursors **6** and **7** show appreciably good to moderate chemoselectivity for aldehydes with each cycle (Fig. 3). The preference for aldehydes is comparable for both catalyst precursors with each cycle, with the best aldehyde chemoselectivity at 78% (Run 2 for both complexes). Beyond the 2nd cycle, the chemoselectivity for aldehydes is observed to decline slowly, ascribed to the formation of iso-octenes being favoured at this stage. This suggests that the active species remains the same with each recycle and some degradation may occur, leading to the slight decline in chemoselectivity.

3.8 *Product-distribution-time studies using 6: Influence of temperature*

The influence of temperature on the product distribution over time was investigated during the hydroformylation of 1-octene at constant pressure of 40 bar using catalyst precursor **6** (Fig. S8). The reactions were carried out over a maximum period of 4 hours, and the reported values for 1-octene represent the number of moles of substrate that are remaining at each respective time interval. At the lowest temperature of this study (75 °C), the number of moles of the substrate decrease steadily over time, Fig. S8a. Increasing the temperature to 85 °C shows a substantial decline of 1-octene in the system over time, with a further increase in temperature to 95 °C resulting in near-perfect depletion of the substrate. Moreover, at a lower temperature of 75 °C, a steady build-up of iso-octenes is observed between 1 hour and 3 hours of the reaction, Fig. S8c. This would be expected as the rate of isomerisation is generally slower at lower temperatures [51,54]. However, as these iso-octenes build-up in the system at 75°C, an optimum level is reached at 3 hours, beyond which a driving force towards conversion of the isomers to branched aldehydes comes into effect, resulting in the observed rapid decline in iso-octenes, from 31.21 mol% to 8.25 mol% at 3 and 4 hours respectively (Fig. S8c). This observation is further supported by the sharp increase in branched aldehydes between 3 and 4 hours of the reaction at 75 °C, from 11.57 mol% to 31.64 mol% respectively, Fig. S8d. At higher temperatures of 85 °C and 95 °C, the rate of isomerisation is

greater immediately from the 1-hour interval (Fig. S8c), a phenomenon that is expected at high temperatures. These iso-octenes decline rapidly as they are immediately converted to branched aldehydes, further substantiating the observed trend depicted in Fig. S8d at the same temperatures of 85 °C and 95 °C. Moreover, the formation of the linear aldehyde (nonanal) with increase in temperature occurs slowly with time (Fig. S8b), as the dominance of the branched aldehydes becomes pronounced due to the high temperatures favouring the double-bond isomerisation of the substrate prior to hydroformylation.

3.9 *Product-distribution-time studies using 6: Influence of pressure*

The influence of pressure on the product distribution over time was investigated during the hydroformylation of 1-octene at constant temperature of 85 °C using catalyst precursor **6** (Fig. S9). It should be mentioned that there was no notable influence on performance of the catalyst when the partial pressure of the CO and H₂ were varied at 85 °C, hence the data reported herein represents that obtained at equimolar ratio of CO:H₂. The lower syngas pressure of 20 bar favours greater accumulation of iso-octenes with time (over two hours) before these can build-up sufficiently enough to create a driving force for their hydroformylation into aldehydes (after 2 hours, Fig. S9c). This driving force is reached earlier at higher pressures (at 1 hour, for 30 and 40 bar, Fig. S9c), allowing for a more improved transformation of these iso-octenes to branched aldehydes between 1 and 4 hours of reaction time. This corresponds well with the observed sudden increase of branched aldehydes from 1 hour of reaction time (Fig. S9d) at the same syngas pressure of 30 and 40 bar.

3.10 *Product-distribution-time studies using 6: Influence of catalyst loading*

The influence of catalyst loading on the product distribution over time was investigated during the hydroformylation of 1-octene at the optimum temperature (85 °C) and pressure (40 bar) using catalyst precursor **6** (Fig. S10). The quantity of 1-octene in the system is observed at comparable levels to the normal and double catalyst loading between 2 hour and 4 hour time intervals (Fig. S10a), which is indicative of a system that has reached the optimum point of influence with respect to the catalyst loading. Interesting to note is the increase in iso-octenes from 1 hour (18.27 mol%) to 2 hours (37.87 mol%) at half catalyst loading (Fig. S10c), indicative of the influence of low

catalyst concentration on lowering the rate of isomerisation. This leads to a slower build-up of iso-octenes, before finally being overcome at a longer reaction time (2–4 hours) via conversion thereof to the branched aldehydes, which is evidently later than that at higher catalyst concentrations, an observation further supported by the profile depicted in Fig. S10d.

A closer look at the chemo- and regioselectivity product distribution profiles using the normal catalyst loading under optimum conditions (85 °C and 40 bar) is shown in Fig. 4. The iso-octenes accumulate during the first hour of reaction, beyond which hydroformylation occurs rapidly, leading to formation of more branched aldehydes.

3.11 Product-distribution-time studies using **7**

The product-distribution-time profile using catalyst precursor **7** for the hydroformylation of 1-octene were evaluated and compared against that of the mononuclear complex **6** at a temperature of 85 °C and a syngas pressure of 20 bar. The kinetics of the trinuclear complex are similar to that of the mononuclear complex (Fig. 5). This behaviour suggests that the metal centres of the trinuclear complex are behaving as a mononuclear entity in the system, which correlates with the catalytic data obtained (vide supra). It is generally accepted that similar reaction kinetics translate to similar rate constants, necessitating the determination of the rate constants of the pre-catalysts based on the data obtained for the mononuclear complex **6**.

3.12 Determination of the reaction rate constants and calculation of activation energy

From the product distribution profiles of the catalyst precursor **6** (based on total aldehydes formed), the observed reaction rate constants (k_{obs}) were then estimated from equation 1 using the least square regression analysis, with first-order dependence in the olefin, shown in Table 4 below.

$$\frac{d(C_{octenes})}{dt} = -k_{obs}C_{octenes} \quad (1)$$

The rate constants agree with the general expectation of the rate of a catalytic reaction increasing with increase in temperature at constant pressure (40 bar, entries 1 to 3). Moreover, at constant temperature (85 °C), varying the pressure results in an increase in the rate constants, indicative of the effect of increased concentration of syngas in the system, from 0.13 h⁻¹ (20 bar, entry 5) to 0.49 h⁻¹ (40 bar, entry 2). The effect of the catalyst loading is also evident on the rate constants at a constant temperature and pressure of 85 °C and 40 bar respectively, increasing from 0.39 h⁻¹ (entry 6, half catalyst loading) to 0.49 h⁻¹ (entry 2, normal catalyst loading) and 0.71 h⁻¹ (entry 7, double catalyst loading). As expected, the influence of temperature on the rate constant is consistent with the Arrhenius Equation (Equation 2).

$$k_{obs} = k_0 e^{\left(\frac{-E}{RT}\right)} \quad (2)$$

From this equation, the activation energy was calculated to be 62 kJ.mol⁻¹. This value is comparable to the ranges obtained using similar rhodium(I) catalysts for the hydroformylation of medium-chain alpha-olefins in a homogeneous solution [59–61].

To further describe the observed rate constants (k_{obs}) in terms of catalyst and syngas pressure effects of Table 4, a fundamental mechanism-based rate law model was applied, as proposed by Dutta and co-workers [61], and shown in Equation 3.

$$\frac{dC_{octenes}}{dt} = -\frac{kC_{Rh}(P_{CO})(P_{H_2})C_8}{1 + K(P_{CO})} \quad (3)$$

However, the rate model did not satisfactorily describe the observed rate constants. This might be due to simplifications of the mechanistic steps used to derive the rate model equation. To obtain a better fit of the observed rate data necessitated modifying the rate model with respect to the catalyst loading, as given in Equation 4.

$$\frac{dC_{octenes}}{dt} = -\frac{kC_{Rh}^{\alpha}(P_{CO})(P_{H_2})C_8}{1 + K(P_{CO})} \quad (4)$$

A summary of the kinetic parameters obtained from Equation 4 are shown in Table 5.

A parity plot of the observed and predicted rate constants was then generated and is shown in Fig. 6.

The parity plot shows that the observed rate constants satisfactorily compare to the calculated mechanism-based model rate constants, in support of the experimental kinetics obtained for the mononuclear complex **6** in the hydroformylation of 1-octene. To the best of our knowledge, there are no reports of kinetic studies on 1-octene using salicylaldimine-based Rh(I) complexes. However, several kinetics on hydroformylation of olefins have been reported in the literature, for both homogeneous and biphasic systems [62–69].

4. Conclusions

New salicylaldimine aryl ether 1,4-substituted 1,2,3-triazole-based complexes have been synthesised. The mononuclear complex **6** was evaluated for optimisation studies in the hydroformylation of 1-octene. Optimum conditions were established at 85 °C, 40 bar for 4 hours. Conversion of the iso-octenes to aldehydes accounts for the regioselectivity towards branched aldehydes at high temperatures. Mercury poisoning experiments using catalyst precursor **6** revealed a nanoparticle mediated transformation of 1-octene. The trinuclear complex posted comparable catalytic conversion and activity to its mononuclear analogue, possible due to the poor solubility of the trinuclear complex in toluene. The mononuclear complex was also evaluated in the hydroformylation of internal olefins 7-tetradecene and 4-octene, with 7-tetradecene giving good chemoselectivity for aldehydes. The complexes **6** and **7** were also evaluated for their recoverability in the hydroformylation reaction of 1-octene using organic solvent nanofiltration (OSN) membrane technology. The complexes could be recycled for at least 5 times with appreciably consistent catalyst performance throughout the cycles, which is significant towards addressing one of the major challenges of designing recoverable and reusable homogeneous hydroformylation catalysts. Kinetic studies were also carried out to determine the rate constants of the hydroformylation of 1-octene using catalyst precursors **6** and **7**, with catalyst precursor **7** posting similar reaction kinetics to catalyst precursor **6**. The reaction rate constants were then calculated based on the mononuclear complex **6** and the activation energy

was determined to be 62 kJ mol⁻¹. The observed reaction rate constants correlated well with a modified fundamental mechanistic-based rate model, validating the experimental kinetics obtained for the mononuclear complex **6** in the hydroformylation of 1-octene.

Acknowledgements

We would like to thank the University of Cape Town (UCT), Stellenbosch University, The Department of Science and Technology of South Africa and NRF-DST Centre of Excellence in Catalysis – c*change for financial support.

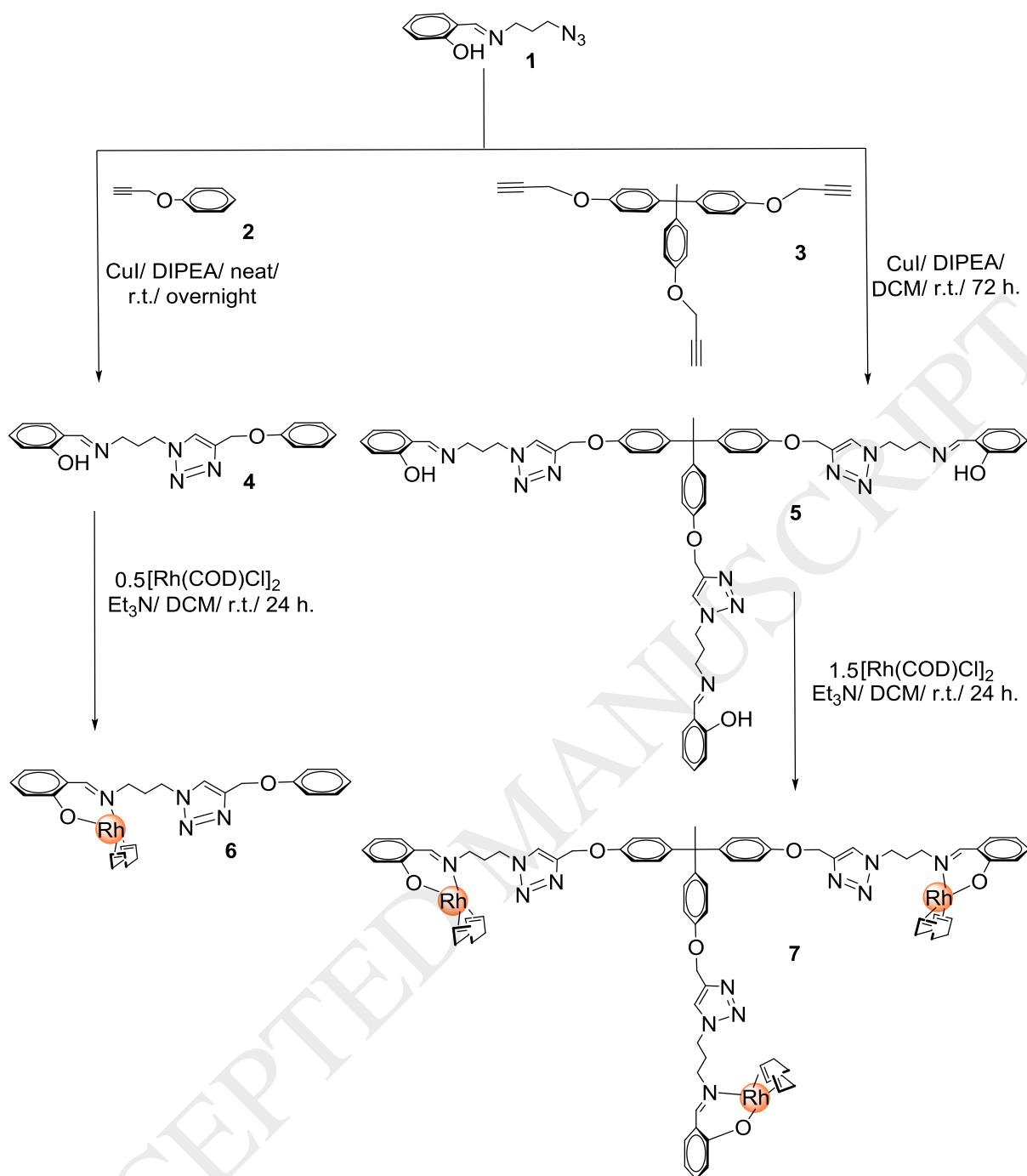
References

- [1] R. Franke, D. Selent, A. Börner, *Chem. Rev.* 112 (2012) 5675–732.
- [2] G.D. Frey, *J. Organomet. Chem.* 754 (2013) 5–7.
- [3] B. Cornils, W.A. Herrmann, M. Rasch, *Angew. Chem. Int. Ed.* 33 (1994) 2144–2163.
- [4] R.L. Pruett, *J. Chem. Educ.* 63 (1986) 196–198.
- [5] B.R. James, P.W.N.M. Van Leeuwen, S.D. Ittel, A. Nakamura, R.L. Richards, A. Yamamoto, in: *Rhodium Catalyzed Hydroformylation*, 1st ed., Kluwer Academic Publishers, New York, 2002, pp. 6–277.
- [6] R. Franke, D. Selent, A. Börner, *Chem. Rev.* 112 (2012) 5675–5732.
- [7] D.J. Cole-Hamilton, R.P. Tooze, *Catalyst Separation, Recovery and Recycling*, Springer, Dordrecht, 2006.
- [8] D. Sharma, V. Ganesh, A. Sakthivel, *Appl. Catal. A, Gen.* 555 (2018) 155–160.
- [9] B. Cornils, *Org. Process Res. Dev.* 1 (1998) 121–127.
- [10] T. Van Vu, H. Kosslick, A. Schulz, J. Harloff, E. Paetzold, M. Schneider, J. Radnik, N. Steinfeldt, G. Fulda, U. Kragl, *Applied Catal. A, Gen.* 468 (2013) 410–417.
- [11] W. Keim, *Green Chem.* 5 (2003) 105–111.
- [12] M. Benaglia, *Recoverable and Recyclable Catalysts.*, 1st ed., John Wiley & Sons, Ltd., Chichester, 2009.
- [13] A.E.C. Collis, I.T. Horváth, *Catal. Sci. Technol.* 1 (2011) 912–919.
- [14] C. De Rumpa, S. Sumanta, A. Ghosh, K. Mukherjee, S. Bhattacharyya, Sekhar, B. Saha, *Res Chem Intermed* 39 (2013) 3463–3474.
- [15] M. Janssen, J. Wilting, C. Müller, D. Vogt, *Angew. Chem. Int. Ed. Engl.* 49 (2010) 7738–41.

- [16] Â.C.B. Neves, M.J.F. Calvete, M.V.D. Pinho, M.M. Pereira, *Eur. J. Org. Chem.* (2012) 6309–6320.
- [17] C. Li, W. Wang, L. Yan, Y. Ding, *Front. Chem. Sci. Eng.* 12 (2018) 113–123.
- [18] E. Vunain, P. Ncube, K. Jalama, R. Meijboom, *J. Porous Mater.* 25 (2018) 303–320.
- [19] I. Vural Gürsel, T. Noel, Q. Wang, V. Hessel, *Green Chem.* 17 (2015) 2012–2026.
- [20] M. Christian, D. Vogt, *Green Chem.* 13 (2011) 2247–2257.
- [21] M. Rabiller-baudry, G. Nasser, T. Renouard, D. Delaunay, M. Camus, *Sep. Purif. Technol.* 116 (2013) 46–60.
- [22] E.L. V Goetheer, A.W. Verkerk, L.J.P. Van Den Broeke, E. De Wolf, B. Deelman, G. Van Koten, J.T.F. Keurentjes, *J. Catal.* 219 (2003) 126–133.
- [23] P. Pemangkin, R.I. Hidridokarboniltris, *Sains Malaysiana* 42 (2013) 515–520.
- [24] E.I.P. De, *J. Mol. Catal.* 2 (1977) 253–263.
- [25] P. Marchetti, M.F.J. Solomon, G. Szekely, A.G. Livingston, *M.S. Equation, Chem. Rev.* 114 (2014) 10735–10806.
- [26] P. Van Der Gryp, A. Barnard, J. Cronje, D. De Vlieger, S. Marx, H.C.M. Vosloo, *J. Memb. Sci.* 353 (2010) 70–77.
- [27] J.T. Scarpello, D. Nair, L.M. Freitas, L.S. White, A.G. Livingston, *J. Memb. Sci.* 203 (2002) 71–85.
- [28] A. Keraani, T. Renouard, C. Fischmeister, C. Bruneau, *ChemSusChem* 1 (2008) 927–933.
- [29] W.E. Siew, C. Ates, A. Merschaert, A.G. Livingston, *Green Chem.* 15 (2013) 663–674.
- [30] K. De Smet, S. Aerts, E. Ceulemans, I.F.J. Vankelecom, P.A. Jacobs, *Chem. Commun.* (2001) 597–598.
- [31] M. Priske, K. Wiese, A. Drews, M. Kraume, G. Baumgarten, *J. Memb. Sci.* 360 (2010) 77–83.
- [32] A. Lejeune, M. Rabiller-baudry, T. Renouard, *Sep. Purif. Technol.* 195 (2018) 339–357.
- [33] P. Schmidt, E. Laura, P. Lutze, A. Górak, *Chem. Eng. Sci.* 115 (2014) 115–126.
- [34] G. Giffels, J. Beliczey, M. Felder, U. Kragl, *Tetrahedron: Asymmetry* 9 (1998) 691–696.
- [35] N. Brinkmann, D. Giebel, G. Lohmer, M.T. Reetz, U. Kragl, *J. Catal.* 168 (1999) 163–168.
- [36] J. Fang, R. Jana, J.A. Tunge, B. Subramaniam, *"Applied Catal. A, Gen.* 393

- (2011) 294–301.
- [37] P.J. Deuss, R. Denheeten, W. Laan, P.C.J. Kamer, *Chem. Eur. J.* 17 (2011) 4680–4698.
- [38] M.H. Pørez-Temprano, J.A. Casares, P. Espinet, *Chem. Eur. J.* 18 (2012) 1864–1884.
- [39] D. Astruc, F. Chardac, *Chem. Rev.* 101 (2001) 2991–3023.
- [40] R.W. Kluiber, G. Sasso, *Inorg. Chim. Acta.* 4 (1970) 226–230.
- [41] P.K. Biswas, S. Saha, T. Paululat, M. Schmittel, *J. Am. Chem. Soc.* 140 (2018) 9038–9041.
- [42] M. Sun, H.Y. Zhang, Q. Zhao, X.Y. Hu, L.H. Wang, B.W. Liu, Y. Liu, *J. Mater. Chem. B* 3 (2015) 8170–8179.
- [43] P. Van Der Gryp, S. Marx, H.C.M. Vosloo, *J. Mol. Catal. A Chem.* 355 (2012) 85–95.
- [44] C. Ornelas, A.K. Diallo, J. Ruiz, D. Astruc, *Adv. Synth. Catal.* 351 (2009) 2147–2154.
- [45] C. Shao, X. Wang, Q. Zhang, S. Luo, J. Zhao, Y. Hu, *J. Org. Chem.* 76 (2011) 6832–6836.
- [46] S. Siangwata, S. Chulu, C.L. Oliver, G.S. Smith, *Appl. Organomet. Chem.* 31 (2017) e3593.
- [47] S. Sun, P. Wu, *J. Phys. Chem. A* 114 (2010) 8331–8336.
- [48] L.C. Matsinha, S.F. Mapolie, G.S. Smith, *Dalton Trans.* 44 (2015) 1240–1248.
- [49] E.B. Hager, B.C.E. Makhubela, G.S. Smith, *Dalton Trans.* 41 (2012) 13927–35.
- [50] L. Maqeda, B.C.E. Makhubela, G.S. Smith, *Polyhedron* 91 (2015) 128–135.
- [51] S. Siangwata, N. Baartzes, B.C.E. Makhubela, G.S. Smith, *J. Organomet. Chem.* 796 (2015) 26–32.
- [52] C. Williams, M. Ferreira, E. Monflier, S.F. Mapolie, G.S. Smith, *Dalton Trans.* 47 (2018) 9418–9429.
- [53] J. October, S.F. Mapolie, *J. Organomet. Chem.* 840 (2017) 1–10.
- [54] N.C. Antonels, J.R. Moss, G.S. Smith, *J. Organomet. Chem.* 696 (2011) 2003–2007.
- [55] L. Le Goanvic, J. Couturier, J. Dubois, J. Carpentier, *Catalysts* 8 (2018) 1–22.
- [56] Y. Yan, X. Zhang, X. Zhang, *J. Am. Chem. Soc.* 128 (2006) 16058–16061.
- [57] M. Haumann, H. Koch, P. Hugo, R. Schomäcker, *Appl. Catal. A Gen.* 225 (2002) 239–249.

- [58] M. Vilches-Herrera, L. Domke, A. Börner, *ACS Catal.* 4 (2014) 1706–1724.
- [59] M.M. Diwakar, R.M. Deshpande, R. V. Chaudhari, *J. Mol. Catal. A Chem.* 232 (2005) 179–186.
- [60] B.M. Bhanage, S.S. Divekar, R.M. Deshpande, R. V. Chaudhari, *J. Mol. Catal. A Chem.* 115 (1997) 247–257.
- [61] M.S. Shaharun, B.K. Dutta, H. Mukhtar, S. Maitra, *Chem. Eng. Sci.* 65 (2010) 273–281.
- [62] R.M. Deshpande, Purwanto, H. Delmas, R. V. Chaudhari, *Ind. Eng. Chem. Res.* 35 (1996) 3927–3933.
- [63] A.C.J. Koeken, L.J.P. Van Den Broeke, B.J. Deelman, J.T.F. Keurentjes, *J. Mol. Catal. A Chem.* 346 (2011) 1–11.
- [64] R.M. Deshpande, A.A. Kelkar, A. Sharma, C. Julcour-Lebigue, H. Delmas, *Chem. Eng. Sci.* 66 (2011) 1631–1639.
- [65] V.K. Srivastava, S.K. Sharma, R.S. Shukla, N. Subrahmanyam, R.V. Jasra, *Ind. Eng. Chem. Res.* 44 (2005) 1764–1771.
- [66] M. Rosales, O. Soto, B. González, I. Pacheco, P.J. Baricelli, *Transit. Met. Chem.* 43 (2018) 451–461.
- [67] N.C.C. Breckwoldt, N.J. Goosen, H.C.M. Vosloo, P. Van der Gryp, *React. Chem. Eng.* (2019) DOI: 10.1039/c8re00239h.
- [68] S. Güven, B. Hamers, R. Franke, M. Priske, M. Becker, D. Vogt, *Catal. Sci. Technol.* 4 (2014) 524–530.
- [69] R. V. Chaudhari, A. Seayad, S. Jayasree, *Catal. Today* 66 (2001) 371–380.



Scheme 1. Synthetic route to aryl-ether Rh(I) mono- and trinuclear complexes **6** and **7**.

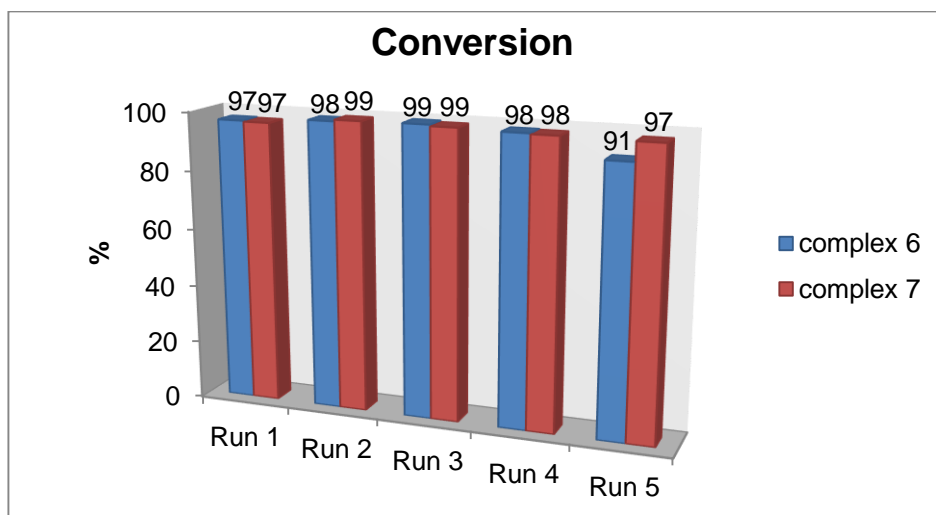


Fig. 1. Percentage conversion of 1-octene during OSN recyclability studies in the hydroformylation of 1-octene.

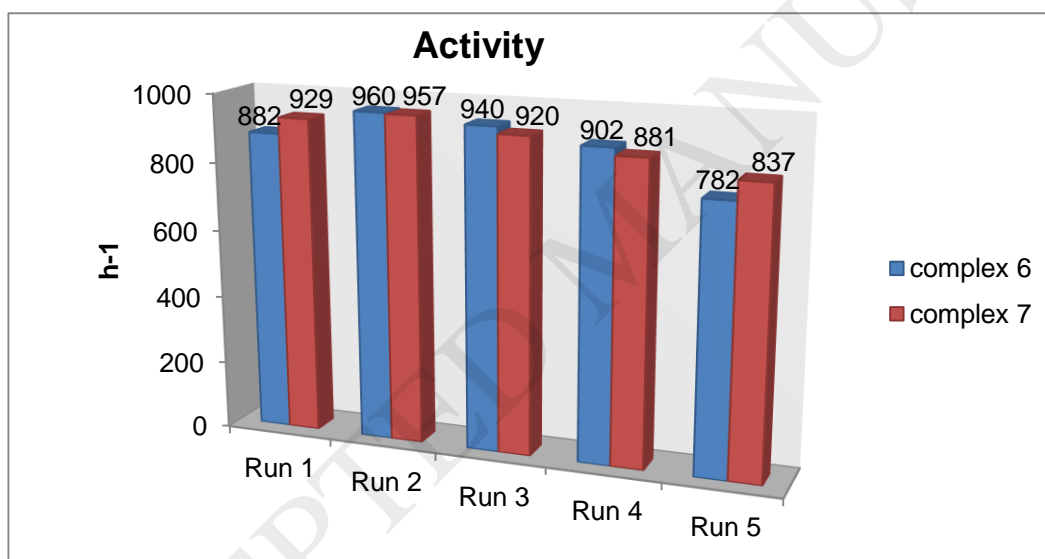


Fig. 2. Activity of the complexes during OSN recyclability studies in the hydroformylation of 1-octene.

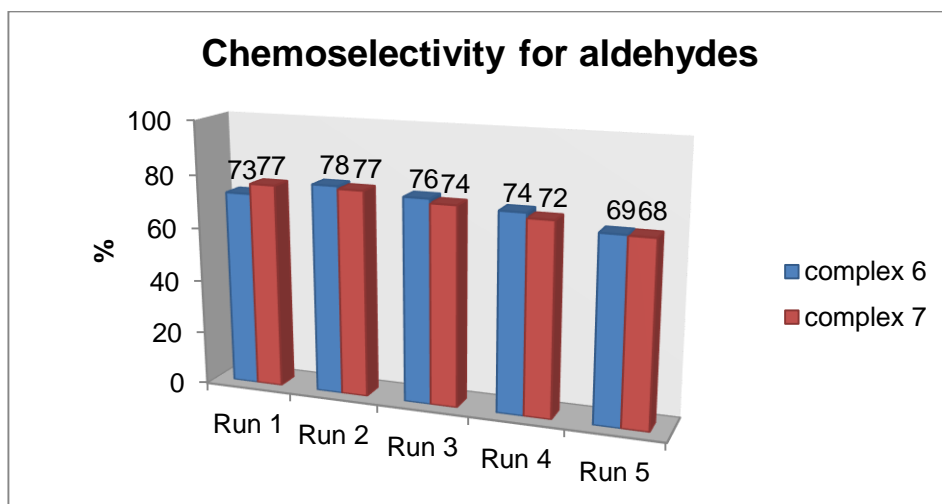


Fig. 3. Chemoselectivity for aldehydes during OSN recyclability studies.

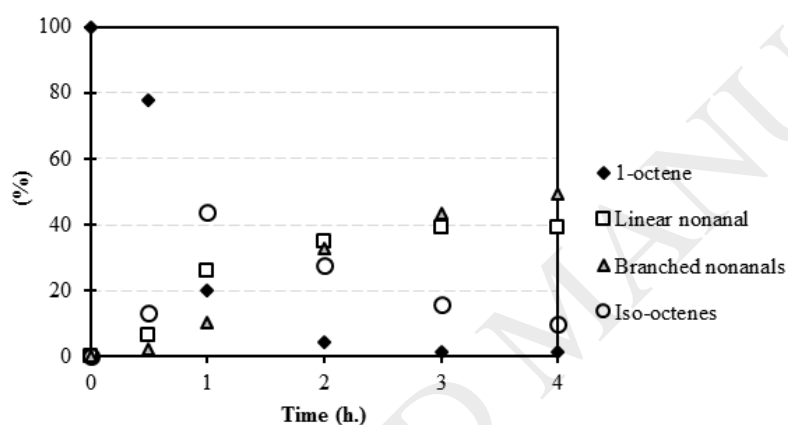


Fig. 4. Substrate and product-distribution-time profile at normal catalyst loading (2.87×10^{-3} mmol of Rh catalyst) and optimum conditions (85 °C /40 bar) with mononuclear complex **6**.

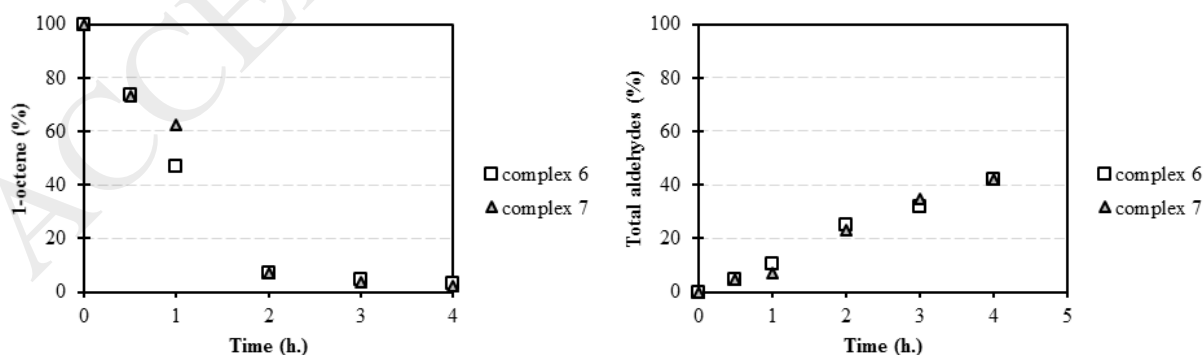


Fig. 5. Substrate and product-distribution-time profiles with the mono- (**6**) and trinuclear (**7**) precatalysts over time.

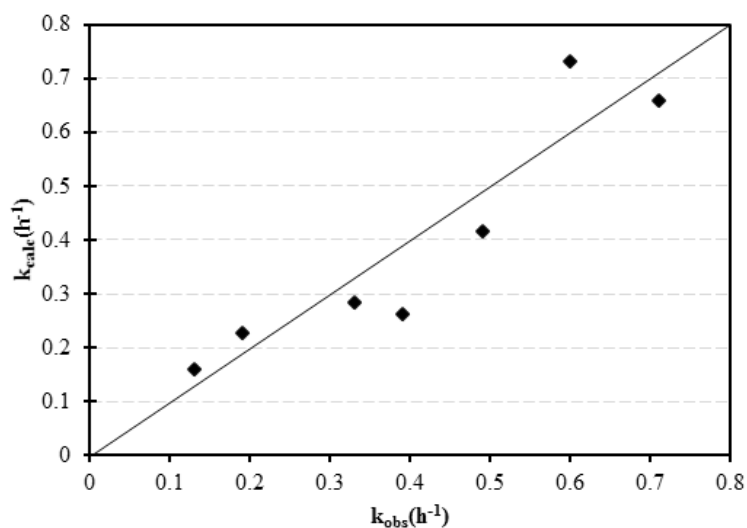


Fig. 6. Parity plot of predicted (k_{calc}) and experimental (k_{obs}) reaction rate constants.

Table 1 Hydroformylation of 1-octene using catalyst precursor **6** for 4 h.^a

Entry	Temp. (°C)	Pressure (bar)	Conv. (%)	Aldehydes (%) ^b	Isoalkenes (%)	<i>n/iso</i> ^c	TOF (h^{-1}) ^d
1	75	20	79	31	69	73:27	154
2	75	30	96	54	46	67:33	323
3	75	40	92	77	23	55:45	444
4	85	20	97	44	56	49:51	264
5	85	30	98	74	26	46:54	454
6	85	40	99	90	10	44:56	554
7 ^e	85	40	93	56	44	63:37	657
8	95	20	99	49	51	39:61	301
9	95	30	99	79	21	39:61	489
10	95	40	99	89	11	40:60	549

^aReactions carried out with syngas (1:1) in toluene (7.5 ml) with 7.175 mmol of 1-octene and 2.87×10^{-3} mmol of Rh catalyst. The reactor was purged with syngas. GC conversions obtained using dodecane as an internal standard in relation to authentic standard iso-octenes and aldehydes. ^bTotal aldehydes formed (from octene and iso-alkenes converted) which includes the primary aldehyde product, nonanal, and isoaldehydes. ^cThe molar ratio of primary linear aldehyde product (*n*) and isoaldehydes (*iso*) formed. ^dTOF = (mmol of aldehydes per mmol of Rh)/time. ^eEntry 7 was conducted in the presence of mercury. Average error estimate = ± 0.68 .

Table 2 Hydroformylation of 1-octene with catalyst precursors **6** and **7** for 4 h.^a

Complex	Temp. (°C)	Pressure (bar)	Conv. (%)	Aldehydes (%) ^b	Isoalkenes (%)	<i>n/iso</i> ^c	TOF (h ⁻¹) ^d
6	85	20	97	44	56	49:51	264
7	85	20	98	43	57	49:51	265

^aReactions carried out with syngas (1:1) in toluene (7.5 ml) with 7.175 mmol of 1-octene and 2.87×10^{-3} mmol of Rh catalyst for **6**, and 9.57×10^{-4} mmol of Rh catalyst for **7**. GC conversions obtained using dodecane as an internal standard in relation to authentic standard iso-octenes and aldehydes. ^bTotal aldehydes formed (from octene and iso-olefins converted) which includes the primary aldehyde product, nonanal, and isoaldehydes. ^cThe molar ratio of primary linear aldehyde product (*n*) and isoaldehydes (*iso*) formed. ^dTOF = (mmol of aldehydes per mmol of Rh)/time. Average error estimate = ± 0.76 .

Table 3 Hydroformylation of internal olefins with catalyst precursor **6** for 4 h.^a

Substrate	Temp. (°C)	Pressure (bar)	Conv. (%)	Aldehydes (%) ^b	Isoalkenes (%)	TOF (h ⁻¹) ^c
7-tetradecene	120	40	85	90	10	841
Trans-4-octene	120	40	92	18	82	102

^aReactions carried out with syngas (1:1) in toluene (7.5 ml) with 7.175 mmol of 1-octene and 2.87×10^{-3} mmol of Rh catalyst for **6**. GC conversions obtained using dodecane as an internal standard in relation to authentic standard iso-octenes and aldehydes. ^bTotal aldehydes formed (from substrate and iso-olefins converted) which includes the primary branched aldehyde product and iso-aldehydes. ^cTOF = (mmol of aldehydes per mmol of Rh)/time. Average error estimate = ± 0.51 .

Table 4 Reaction rate constants of catalyst precursor **6**.

Entry	Temp. (°C)	P_{Total} (bar)	Catalyst load	k_{obs} (h ⁻¹)
1	75	40	Normal	0.19
2	85	40	Normal	0.49
3	95	40	Normal	0.60
4	85	30	Normal	0.33
5	85	20	Normal	0.13
6	85	40	Half	0.39
7	85	40	Double	0.71

Normal catalyst loading = 2.87×10^{-3} mmol of Rh catalyst, half catalyst loading = 1.44×10^{-3} mmol of Rh catalyst, and double catalyst loading = 5.74×10^{-3} mmol of Rh catalyst.

Table 5 Summary of the rate model parameters.

Parameter	Value
k_0 (L ^{α} mol ^{-α} bar ² h ⁻¹)	5.64×10^8
E_A (kJ.mol ⁻¹)	62
K (bar ⁻¹)	0.12

α	0.7
----------	-----

ACCEPTED MANUSCRIPT